Time Series Prediction of Respiratory Motion for Lung Tumor Tracking Radiation Therapy

NORIYASU HOMMA
Tohoku University
Cyberscience Center
6-6-05 Aoba, Aoba-ku
Sendai 980-8579
JAPAN
homma@ieee.org

MASAO SAKAI
Tohoku University
Center for Advancement of Higher Education
41 Kawauchi, Aoba-ku
Sendai 980-8576
JAPAN
sakai@he.tohoku.ac.jp

YOSHIHIRO TAKAI
Tohoku University
Graduate School of Medicine
2-1 Seiryo-machi, Aoba-ku
Sendai 980-8575
JAPAN
y-takai@mail.tains.tohoku.ac.jp

Abstract: A time series prediction problem is considered in this paper. In radiotherapy, the target motion often affects the conformability of the therapeutic dose distribution delivered to thoracic and abdominal tumors, and thus tumor motion monitoring systems have been developed. Even we can observe tumor motion accurately, however, radiotherapy systems may inherently have mechanical and computational delays to be compensated for synchronizing dose delivery with the motion. For solving the delay problem, we develop a novel system to predict complex time series of the lung tumor motion. An essential core of the system is an adaptive prediction modeling by which time-varying cyclic dynamics is transferred into time invariant one by a phase locking technique. After the transformation, some linear and nonlinear models including neural networks can be used for accurate time series prediction. Simulation studies demonstrate that the proposed system can achieve a clinically useful high accuracy and long-term prediction of the average error 1.59 ± 1.61 [mm] at 1 [sec] ahead prediction.

Key–Words: Time series prediction, adaptive modeling, radiation therapy, and motion management.

1 Introduction

In radiation therapy, it is known that the target motion often affects the conformability of the therapeutic dose distribution delivered to thoracic and abdominal tumors. Such tumor motions can not only be associate with patient's stochastic movements and systematic drifts, but also involve internal movements caused by such as respiration and cardiac cycles [1].

To take into account such "dynamic" nature of the internal organ motion during the course of radiation therapy, several techniques have been proposed and evaluated in clinical use. A simple method is to increase the planning target volume (PTV) to cover the possible range of motion of the target [2], but undesirably it results in an increased dose to the normal tissues surrounding the tumor. One of the other methods to treat the respiratory motion of the lung tumor is a breath-hold technique [3]. Since the respiration may be dominant over the lung tumor motion, the tumor can be regarded as a static target by using such technique to stop the respiration. Geometric gating method is also this kind of techniques to limit the motion effect [4, 5]. They are, however, not desirable techniques because of patient intervention by the breath-hold or beam interruption by the gating. In this sense, tumor tracking by moving the radiation source [6, 7] or the beam defined by multileaf collimator [8] can be in an ideal direction.

To achieve such tumor tracking, several methods have been proposed. Among these, direct measurements of the tumor position by fluoroscopy imaging techniques [9, 10] are more promising than indirect ones such as external skin marker tracking [5, 11] and breath monitoring techniques [12]. Such tracking systems may involve mechanical and computational delays to control the multileaf collimator and for image and time series processings of the tumor motion. Thus, the time delay must be compensated by predicting the tumor motion to accomplish a real-time tracking [1]. The desired accuracy of the tumor location can be within about 1 [mm] at up to 1 [sec] ahead prediction. This is a highly accurate condition for the complex dynamics of the tumor motion.

In this paper, we propose a new system realizing such highly accurate prediction of lung tumor motion for tracking radiation therapy. The proposed system takes into account the complex dynamics by using an adaptive modeling for the prediction.

The rest of this paper consists of as follows. We will investigate nature of the motion first, by using time series analysis techniques in section II. Then prediction method will be developed in section III by

using results of the analysis. In section IV, prediction accuracy of the proposed system will be evaluated by some simulation studies in which the performance of the prediction systems based on a smoothing prediction model designed by Holt-Winters seasonal (HWS) method [13] and more general seasonal ARIMA (SARIMA) model [14] is compared to a conventional prediction method. Concluding remarks will be given in section V.

2 Motion of Lung Tumor

We used three-dimensional time series of human lung tumor motion at superior segment of right lung, S6, as shown in Fig. 1. A dominant source of the tumor motion is respiration, but the others such as caused by cardiac motion may also be included in the time series.

2.1 Preprocessing (noise reduction) of the time series

A fiducial gold marker implanted into the lung tumor was used to measure the three-dimensional coordinates of the tumor motion. The spatial resolution and sampling period were 0.01[mm] and 0.033[sec] (30[Hz]), respectively. To reduce observational noise and avoid abnormal data involved in raw data of the time series, we preprocessed the time series by using several filters such as the Kalman filter [15] and statistical filters. An example of the preprocessed time series

$$\boldsymbol{y}(t) = [y_1(t)\ y_2(t)\ y_3(t)] \qquad (1)$$

$t = 1, 2, \ldots, 5000$, are shown in Fig. 2. Here elements of vector $\boldsymbol{y}(t)$ at time t [step], $y_1(t), y_2(t)$, and $y_3(t)$ [mm], are the marker's position of the sagittal, axial, and coronal directions, respectively. Note that

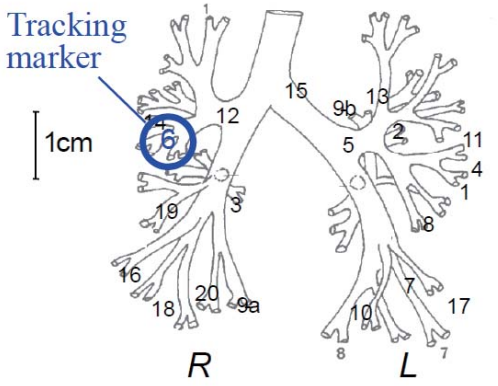

Figure 1: Structure of a human lung.

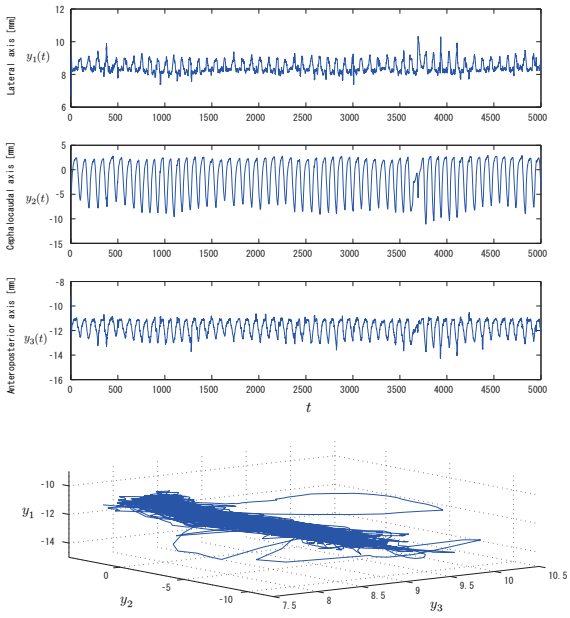

Figure 2: Preprocessed time series $\boldsymbol{y}(t)$ of the observed tumor marker motion at S6 of the lung.

the time series of the vector $\boldsymbol{y}(t)$, $t = 1, 2, ...$, can be obtained in real-time.

For the teaching data of time series prediction, we further reduced the observational impulse noise involved in the time series $\boldsymbol{y}(t)$, $t = 1, 2, ...$, in Eq. (1) by using statistical filters, and then reduced high frequency noise by using a low pass filter that deletes unnecessary high frequency components that are higher than $0.1 \times f_{\max}$ [Hz]. Here $f_{\max}$ is the maximum frequency of the digital Fourier transform spectrum under the sampling period. The statistics can be computed by using all data of the time series for $t = 1, 2, \ldots, 5000$ in Fig. 2. The noise reduced time series $\boldsymbol{y}^*(t) = [y_1^*(t)\ y_2^*(t)\ y_3^*(t)]$ are shown in Fig. 3 and assumed as the real motion of the fiducial marker of the tumor.

2.2 Cyclic dynamics

There can be cyclic dynamics with approximately 90 [steps] periods of respiratory motion involved in the fiducial marker motion of the lung tumor as seen in Figs. 2 and 3. Note that the periods of the cyclic components and rhythmic dynamics can be widely fluctuated when the respiratory dynamics are changed. If patients are in rest, however, respiratory dynamics is almost cyclic and thus the dominant dynamics of time series is also cyclic as seen in Fig. 2.

We calculate the autocorrelation function, ACF, of the time series for further analysis of the cyclic dynamics involved in the tumor motion. Fig. 4 shows ACF(t, k) of a sample time series in the axial direc-

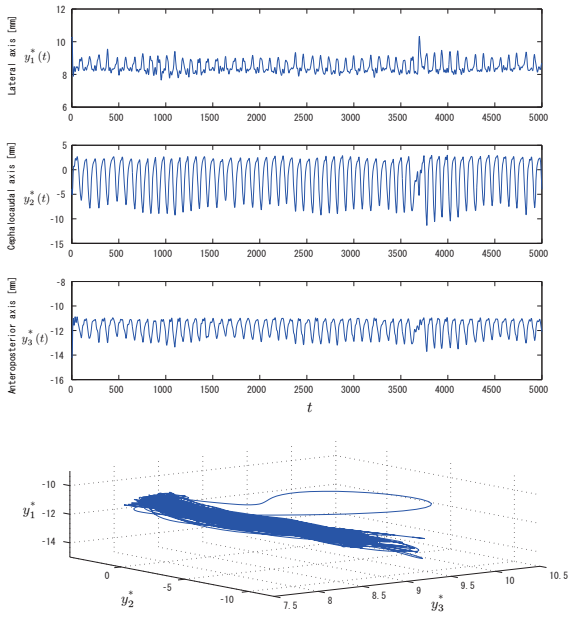

Figure 3: The noise reduced time series $\boldsymbol{y}^*(t)$ of the marker motion.

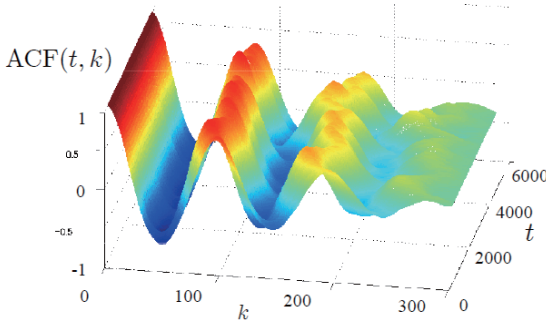

Figure 4: Autocorrelation function, $\mathrm{ACF}(t,k)$, of y_2^*.

tion, $[y_2^*(t-150)\ y_2^*(t-149)\ \cdots\ y_2^*(t+149)\ y_2^*(t+150)]$, within a time window (301 steps) as a function of time t [step] and the shift k [step]. Note that the first peak of the ACF at a shift $k(\geq 1)$ corresponds to the dominant period of the cyclic dynamics. Then from the autocorrelation function analysis, it is revealed that the dominant periods are also approximately 90 [steps]. Furthermore, the periods are slightly and smoothly fluctuated and thus they can be time variant. It has been seen that ACFs for time series of the other two directions, y_1^* and y_3^*, are almost similar to that of y_2^* described above (The results are omitted).

3 Prediction Method

3.1 Concept of prediction algorithm

Fig. 5 shows a tumor motion prediction system proposed in this paper. Let us predict the h-step ($h \geq 1$) ahead fiducial marker's position of the lung tumor. The predicted position $\tilde{\boldsymbol{y}}^*(t+h)$ of the actual (noise reduced) tumor position $\boldsymbol{y}^*(t+h)$ is calculated by using the real-time preprocessed time series available at time t

$$\boldsymbol{Y}(t) = [\boldsymbol{y}(1)\ \boldsymbol{y}(2)\ \cdots \boldsymbol{y}(t-1)\ \boldsymbol{y}(t)]^T \qquad (2)$$

Concepts of the prediction algorithm are as follows. As analyzed in section 2.2, the target time series $\boldsymbol{y}^*(t)$ may include a complex dynamics with time variant periods. Thus, far past information involved in the whole time series $\boldsymbol{Y}(t)$ is less important or even can have a bad effect on the prediction accuracy. Then, the prediction model can be built based on the not far past information of the time series. Note that the current period is one of the most important piece of information for the prediction because the cyclic dynamics makes the prediction be precise. In this sense, the proposed algorithm tries to estimate the current dominant period as precise as possible by using a flesh piece of information involved in the current time series available.

Let us consider the current period vector $\boldsymbol{s}^*(t) = [s_1^*(t)\ s_2^*(t)\ s_3^*(t)]$ of the time series $\boldsymbol{y}^*(t) = [y_1^*(t)\ y_2^*(t)\ y_3^*(t)]$ at time t, and denote its estimation as $\boldsymbol{s}(t) = [s_1(t)\ s_2(t)\ s_3(t)]$. The estimation of the $\boldsymbol{s}^*$ can be calculated by using the autocorrelation function analysis of a flesh sample time series with a time length L given as $y_i(\tau), \tau = t-L, t-L+1, \ldots, t$, available at time t. Here if the estimated period is changed, $s_i(t-1) \neq s_i(t)$, then the model of cyclic dynamics is adapted to the new current period $s_i(t)$. The final h-step ahead prediction $\tilde{\boldsymbol{y}}^*(t+h)$ can be calculated based on the adapted model of the new cyclic dynamics $\hat{\boldsymbol{Y}}(t)$ as shown in Fig. 5.

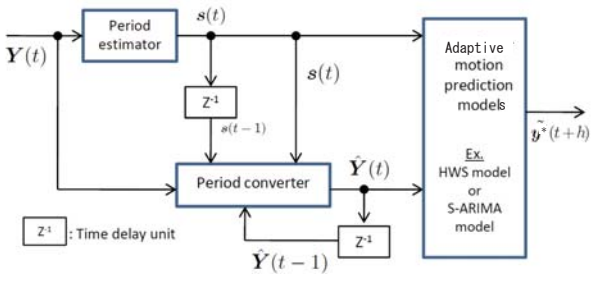

Figure 5: The proposed prediction system.

3.2 Prediction model

As prediction models of the lung tumor motion, we adopt two models of the time series here. One is a smoothing model designed by the HWS method and the other is a seasonal ARIMA (SARIMA) model. Note that, however, any other linear or nonlinear models including neural networks can be used for the proposed adaptive prediction method.

The HWS method can provide an easy design of the model to predict 1-step ahead of the time series if the period of cyclic dynamics is known and time invariant. In such case, only three smoothing parameters, implying the ratio of use the predicted data to the previous actual data for smoothing, may be designed as values between 0 and 1; 0 implies smoothing by only the actual data, while 1 implies smoothing by only the predicted data. The three parameters, $0 \leq \alpha, \beta, \gamma \leq 1$, are ratios for smooth calculation of the trend level, the gradient of trend, and cyclic component, respectively.

On the other hand, the easy design restricts freedom of the model and thus the prediction accuracy is limited in the case of complicated time series. Also, modeling errors may be accumulated for a mid- or long-term prediction ($h \gg 1$) and the prediction will result in failure with a large error beyond the tolerance.

The other model, the general SARIMA model of the time series, $[y(0)\ y(1)\ \cdots\ y(t)]$, with period s [steps] of cyclic dynamics can be given as follows.

$$\phi(B)\Phi(B^s)(1-B)^d(1-B^s)^D y(t) = \theta(B)\Theta(B^s)e(t) \tag{3}$$

$$\begin{aligned}
\phi(x) &= 1 - \phi_1 x - \phi_2 x^2 - \cdots - \phi_p x^p \\
\Phi(x) &= 1 - \Phi_1 x - \Phi_2 x^2 - \cdots - \Phi_P x^P \\
\theta(x) &= 1 + \theta_1 x + \theta_2 x^2 + \cdots + \theta_q x^q \\
\Theta(x) &= 1 + \Theta_1 x + \Theta_2 x^2 + \cdots + \Theta_Q x^Q
\end{aligned}$$

where $e(t)$ is the Gaussian noise of which average and variance are 0 and σ^2, respectively. The parameters d, D, p, P, q, and Q represent dimensions of corresponding terms, respectively. Because of high degree of design parameter freedom of the SARIMA model, the model can predict complicated dynamics with a high precision. It is often, however, hard to design such appropriate parameters of the model for the precise prediction.

To design the SARIMA model, we first make a compensated time series $\boldsymbol{x}(t)$ from the adapted preprocessed time series $\hat{\boldsymbol{y}}(t)$ as

$$\boldsymbol{x}(t) = \hat{\boldsymbol{y}}(t) - \boldsymbol{z}(t) \tag{4}$$

where $\boldsymbol{z}(t) = [z_1(t)\ z_2(t)\ z_3(t)]$ is a trend level vector at time t of the time series $\hat{\boldsymbol{y}}(t)$ defined by

$$z_i(t) = \frac{1}{s_i(t)} \sum_{\tau=t-s_i(t)+1}^{t} \hat{y}_i(\tau) \tag{5}$$

$i = 1, 2, 3$. Then, the SARIMA model can be build by using the compensated time series with a time length of L given as

$$\boldsymbol{X}(t) = [\boldsymbol{x}(t-L)\ \boldsymbol{x}(t-L+1)\ \cdots\ \boldsymbol{x}(t)]^T \tag{6}$$

For avoiding the accumulation of the modeling error at each step, we directly design an h-step ahead prediction model instead of repeatedly use of the 1-step ahead prediction one. To this end, the following constraint can be introduced.

$$\phi_i \quad = \quad 0 \cdots \text{if } \mathrm{mod}(i, [h/2]) \neq 0 \tag{7}$$

where $[x]$ denotes an operator that gives maximum integer not greater than x and $\mathrm{mod}(i, k)$ gives the remainder on division of i by k.

4 Results and Discussions

We have tested the proposed system using a prediction task in which the preprocessed time series $\boldsymbol{Y}(t)$ of fiducial marker's motions of several lung tumors are used. To evaluate the performance under the worst (longest-term) condition required in clinical use, the maximum length of $h = 30$-step (1 [sec]) ahead prediction was conducted first.

The estimation of the current dominant periods of cyclic dynamics was conducted during prediction for the model adaptation. The estimation results are shown in Fig. 6. As seen in this figure, estimated periods as functions of time converge in around 90 after 1000 steps, but are still fluctuated and slightly different from with each other directions. A reason why such long (1000) steps were needed for convergence of the estimated periods may be due to the limitation of the changes of the estimated periods given as $|s_i(t) - s_i(t-1)| \leq 1,\ i = 1, 2, 3$, with the initial values $s_i(0) = 1$ to avoid undesirable oscillation of the estimation by radical changes of the estimation. This may, however, require only additional 30 [sec] observations before the actual therapeutic irradiation in clinical use.

An example of the resulting time series for $t = 3000$ to 5000 predicted by the adaptive smoothing model designed by the HWS method is shown in Fig. 7. In this result, the smoothing parameters were experimentally designed as $\alpha = 0.01,\ \beta = 0.05$, and $\gamma = 0.7$, respectively.

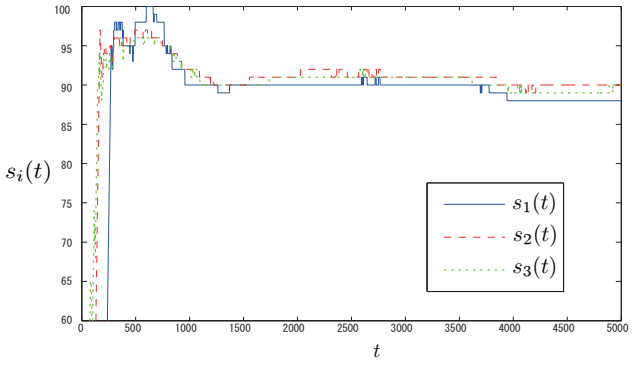

Figure 6: Fluctuation of periods $s_i(t)$, $i = 1, 2, 3$.

On the other hand, for the same target time series, the prediction result by the adaptive SARIMA model is shown in Fig. 8. Here, the dimensional parameters were experimentally designed as $p = 5h, P = 6s_i(t), d = 0, D = 0, q = 0$, and $Q = 0$, respectively. Referential time series predicted by the zero-order hold model given as $\tilde{\boldsymbol{y}}^*(t+h) = \boldsymbol{y}(t)$ are also shown in Figs. 7 and 8. Note that the parameters of both models can be optimized by using some criteria such as Akaike's Information Criterion (AIC) [16].

As is clear from these figures, it can be concluded that prediction accuracy of both smoothing and SARIMA adaptive models is superior to that of

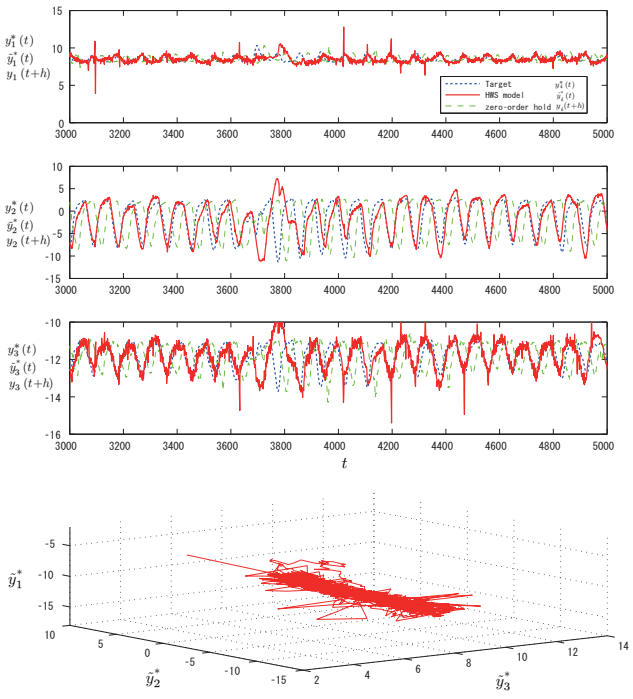

Figure 7: Comparison of time series between the target (blue dotted lines) and the predictions (red lines) at 1 [sec] (30 steps) ahead by the proposed system with HWS model.

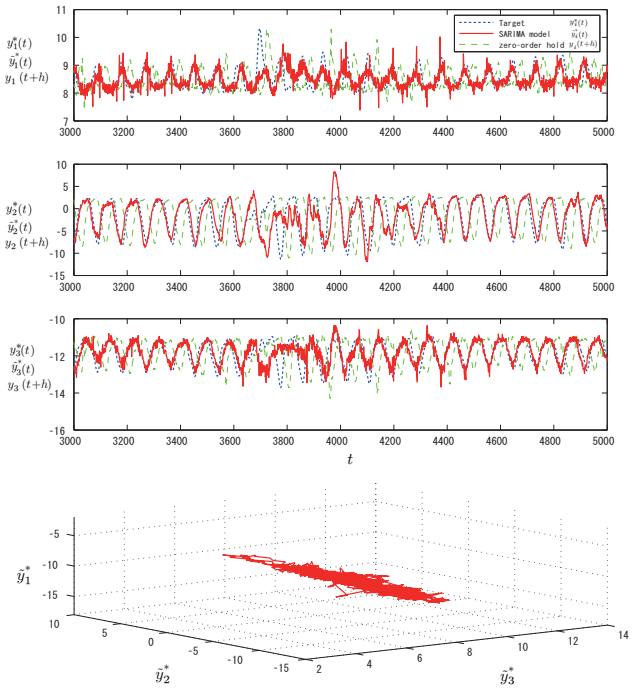

Figure 8: Comparison of time series between the target (blue dotted lines) and the predictions (red lines) at 1 [sec] (30 steps) ahead by the proposed system with SARIMA model.

the zero-order hold model and the SARIMA model is slightly further superior to the smoothing model. This can be the effect of real-time adaptation of the model according to the estimated time variant period and the adaptation is effective even for the simple smoothing model.

In addition, due to nonlinear nature of the respiratory motion, better performance for *short-term predictions* by neural network models compared to linear filters has been reported [17, 18]. Consequently, much better performance for *long-term predictions* can be expected by using any nonlinear models including neural networks with the proposed adaptation algorithm for time variant nature.

To further verify this effect of adaptation, we have evaluated average prediction errors for various h-step ($1 \leq h \leq 40$) ahead prediction tasks. For a wide range of h, prediction accuracy of both the smoothing and SARIMA models was superior to that of the zero-order hold model as expected (The results are omitted). The average error and its standard deviation of the 30-step ahead prediction were 1.94 ± 1.93 [mm] by the smoothing model, while they were 1.59 ± 1.61 [mm] by the SARIMA model. What should be stressed here is that this accuracy can be sufficient for clinical use in which the margin of the dose distribution is less than several millimeters.

5 Conclusions

In this paper, we have developed time series prediction system for lung tumor motion tracking radiation therapy. The precise prediction was achieved by the proposed technique based on the real-time adaptation to the time variant period involved in the cyclic dynamics of respiration that may be a dominant source of the tumor motion. It is expected that such precise prediction will reduce the adverse dosimetric effect of the tumor motion.

Simulation studies revealed the superior prediction performance of the proposed adaptation models compared to the conventional zero-order hold model and that the prediction accuracy may be sufficient for the clinical use. In addition to this, although results were not shown in this paper, the performance of the proposed adaptive SARIMA model was further superior to that of the conventional SARIMA model without the adaptation.

Acknowledgements: This work was partially supported by The Ministry of Education, Culture, Sports, Science and Technology under Grant-in-Aid for Scientific Research #19500413.

References:

[1] M. J. Murphy, "Tracking Moving Organs in Real Time," *Seminars in Radiation Oncology*, vol. 14, no. 1, pp. 91-100, 2004.

[2] M. van Herk, "Errors and margins in radiation oncology," Semin. Radiat. Oncol. vol. 14, pp. 52-64, 2004.

[3] J. Hanley *et al.*, "Deep inspiration breath-hold technique for lung tumors: The potential value of target immobilization and reduced lung density in dose escalation," *Int. J. Radiat. Oncol., Biol., Phys.* vol. 45, pp. 603-611, 1999.

[4] H. D. Kubo *et al.*, "Breathing-synchronized radiotherapy program at the University of California Davis Cancer Center," *Med. Phys.*, vol. 27, pp. 346, 2000.

[5] N. Wink *et al.*, "Individualized gating windows based on fourdimensional CT information for respiration gated radiotherapy," *Med. Phys.*, vol. 34, pp. 2384, 2007.

[6] A. Schweikard *et al.*, "Robotic motion compensation for respiratory movement during radiosurgery," *Comput. Aided Surg.*, vol. 5, pp. 263-277, 2000.

[7] C. Ozhasoglu, "Synchrony-Real-time respiratory compensation system for the CyberKnife," *Med. Phys.*, vol. 33, pp. 2245-2246, 2006.

[8] P. J. Keall *et al.*, "Motion adaptive x-ray therapy: A feasibility study," *Phys. Med. Biol.*, vol. 46, pp. 1-10, 2001.

[9] H. Shirato *et al.*, "Real-time tumor-tracking radiotherapy," *Lancet*, vol. 353, pp. 1331-1332, 1999.

[10] Y. Takai *et al.*, "Development of a new linear accelerator mounted with dual fluoroscopy using amorphous silicon flat panel X-ray sensors to detect a gold seed in a tumor at real treatment position," *Int. J. Radiat. Oncol. Biol. Phys.*, vol. 51 (Supple.), pp. 381, 2001.

[11] C. Ozhasoglu and M. J. Murphy, "Issues in respiratory motion compensation during external-beam radiotherapy," *Int. J. Radiat. Oncol., Biol., Phys.*, vol. 52, pp. 1389-1399, 2002.

[12] L. Simon *et al.*, "Lung volume assessment for a cross-comparison of two breathing-adapted techniques in radiotherapy," *Int. J. Radiat. Oncol., Biol., Phys.*, vol. 63, pp. 602-609, 2005.

[13] P. R. Winters, "Forecasting Sales by Exponentially Weighted Moving Averages," *Management Science*, vol. 6 pp. 324-342, 1960.

[14] G. E. P. Box, G. M. Jenkins, *Time Series Analysis, Forecasting and Control*, Holden-Day, pp. 1-553, 1970.

[15] R. E. Kalman, "A New Approach to Linear Filtering and Prediction Problems," *T. ASME, J. Basic Engineering*, Series D, vol. 83, pp. 35-45, 1961.

[16] K. Akaike and G. Kitagawa, *Practice in Time Series Analysis I*, Asakura-Shoten, 2003 (in Japanese).

[17] M. Isaksson *et al.*, "On using an adaptive neural network to predict lung tumor motion during respiration for radiotherapy applications," *Med. Phys.*, vol. 32, no. 12, pp. 3801-3809, 2005.

[18] M. J. Murphy and S. Dieterich, "Comparative performance of linear and nonlinear neural networks to predict irregular breathing," *Phys. Med. Biol.*, vol. 51, pp. 5903-5914, 2006.